TẠP CHÍ ISSN: 1859-316X, e-ISSN: 3093-3161
KHOA HỌC CÔNG NGHỆ HÀNG HẢI
JOURNAL OF MARINE SCIENCE AND TECHNOLOGY

CFD AND EFD INVESTIGATION ON SHALLOW WATER RESISTANCE

NGHIÊN CỨU LỰC CẢN TÀU TRONG VÙNG NƯỚC NÔNG SỬ DỤNG PHƯƠNG PHÁP CFD VÀ EFD

LE THANH BINH[1*], DO TAT MANH[2]

[1]Maritime Research Institute, Vietnam Maritime University
[2]Institute of Postgraduate Education, Vietnam Maritime University
**Corresponding email: binhlth@vimaru.edu.vn*
DOI: https://doi.org/10.65154/jmst.2025.i84.846

Tóm tắt

This paper presents an investigation on the shallow water resistance of the combatant DTMB 5415 by using CFD techniques and compares its results with experimental data. In this research, the ship's model was used without appendages and simulated at various speeds. The results of the simulation were compared with data from towing tank tests at CTO, Poland.

The simulation results demonstrate the accuracy of the CFD method and its applicability as an effective tool to replace model tests in the design stages, thereby reducing time and costs.

Từ khóa: *CFD, shallow water resistance, morphing mesh, DTMB 5415.*

Abstract

Bài báo trình bày nghiên cứu tính toán lực cản nước nông cho tàu chiến DTMB 5415 sử dụng phương pháp CFD và so sánh kết quả với kết quả thực nghiệm. Trong nghiên cứu, mô hình tàu sử dụng trong mô phỏng không bao gồm các phần nhô với các tốc độ khác nhau. Kết quả được xác thực bằng cách so sánh với dữ liệu có sẵn từ các thử nghiệm tại bể thử mô hình tàu thủy CTO, Ba Lan.

Các kết quả mô phỏng cho thấy độ chính xác của phương pháp CFD và khả năng ứng dụng của nó như một công cụ hiệu quả thay thế thử mô hình trong thiết kế, giúp giảm thời gian và chi phí.

Keywords: *CFD, lực cản nước nông, lưới biến dạng, DTMB 5415.*

1. Introduction

CFD techniques are especially useful in ship hydrodynamics problems, including ship resistance in shallow and confined water. While towing tank tests provide better absolute accuracy, CFD techniques provide the designers another approach with reasonably accurate results at a lower cost and time. The CFD technique is especially useful for optimizing the ship hull by calculating and analyzing different variants quickly and selecting the best variant for verification by the model test [1].

A ship exhibits drastically different behavior when moving in deep water in comparison with shallow water, especially its hydrodynamic wake and wave systems. Recent years have seen numerous research initiatives examining ship hydrodynamics using CFD techniques to solve practical hydrodynamic issues that enable vessels to safely sailing. Accurate determination of the ship's resistance and its floating position are key factors in the accuracy of determining the power of the propulsion system in the early design stage [2]. The influence of shallow water, as well as the limitation of the canal dimensions, can be determined by theoretical methods and regression calculation methods based on the results of model tests. Methods for assessing the influence of depth include: Lackenby - shallow water speed loss assessment, which was recommended by ITTC for use in ship trial procedures; Hoffman and Kozarski charts, including the critical speed region, with satisfactory agreement with experimental data [4]. Besides that, CFD methods have been utilized for studying shallow water resistance for many years. The methods can be found in the work of Pritam Kumar Patel & M. Prechand, Senthil Prakash & Binod Chandra [2], [3].

Figure 1. DTMB 5415 model

This research applies CFD method to determine the shallow water resistance of DTMB 5415. The study compared the bare hull resistance findings with results obtained from the CTO model towing tank in

Poland. This report utilized the DTMB M992 model as shown in Figure 1.

2. Basic theory

2.1. The CFD solver

The STAR CCM+ software was used in the present study. The purpose is to predict the shallow water resistance of DTMB 5415 and demonstrate the capability of the RANSE solver in solving ship resistance in shallow water.

For the simulation, the SST k-omega turbulence model was used. This model combines the advantages of the k-omega and k-epsilon models by using a blending function, allowing its application for a wide range of hydrodynamic simulations [5].

The VOF model was implemented in the simulation to solve the free surface problems, which relate to the water wave surface created by the ship's motions [6].

2.2. Shallow water resistance

Ship resistance in shallow water can differ greatly from deep water in both the value and the wave pattern (Figures 2&3). The shallow water ship resistance could also be separated into parts due to friction and wave-making. However, the value of both parts is distinct from that corresponding to deep water. When a ship moves in the water of finite depth, the value of wave resistance varies both with Fn and the Depth Froude number F_h.

$$F_h = \frac{V}{\sqrt{gh}} \quad (1)$$

Where: V- Ship speed, m/s; h - Water depth, m.

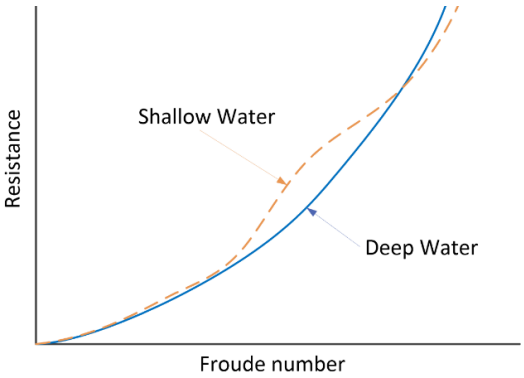

Figure 2. Typical graph of ship resistance in deep and shallow water

For the ship resistance in shallow water, the ship speed is generally divided into three different regions:

- $F_h < 0.6$: "sub-critical" speed range, which has a small difference in comparison with deep water resistance.

- F_h = 0.6~1.2: "near critical" speed range. The ship's resistance reaches a maximum value at a critical speed corresponding to $F_h = 1.0$.

- $F_h > 1.2$: "super-critical" speed range, at which the ship's resistance drops significantly, even smaller than that in deep water.

Ship speed determines the wave pattern in shallow water, which can be either sub-critical, critical, or super-critical. Transverse and divergent waves become visible when the ship operates below the critical speed region with Fh values less than 1. Upon reaching critical speed, when Fh becomes equal to 1, the waves move in a direction perpendicular to the ship's course. When ships travel faster than critical speed in super-critical regions where Fh exceeds 1, divergent waves return along the ship's path at certain angles without visible transverse waves [2].

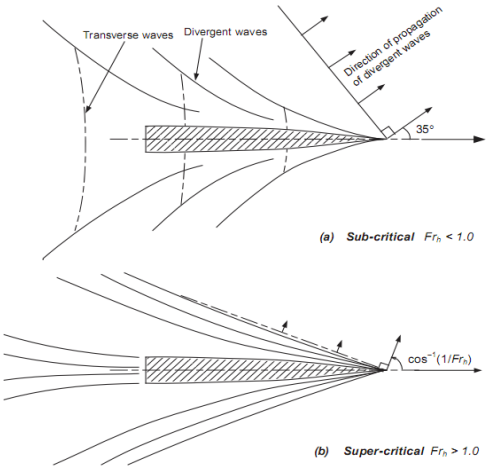

Figure 3. Shallow water wave pattern for different speeds

3. Numerical simulation

Computations were performed for shallow water with 0.46 m water depth ($h/T=2.0$).

The following assumptions were used in simulation modeling: Linear motion with constant speed; Computation with free surface; Ship is considered without appendages; Flat seabed bottom without natural irregularities.

3.1. Hull Geometry

The DTMB 5415 is a twin-propeller surface combatant that was designed in the 1980s. There is no

TẠP CHÍ ISSN: 1859-316X, e-ISSN: 3093-3161
KHOA HỌC CÔNG NGHỆ HÀNG HẢI
JOURNAL OF MARINE SCIENCE AND TECHNOLOGY

Table 1. Hull particulars

Description	Symbol	Ship	Model
Scale factor	λ	-	26.69
Length between perpendicular	L_{PP} (m)	142.00	5.320
Length of waterline	L_{WL} (m)	142.18	5.327
Breadth	B (m)	18.90	0.714
Draft	T (m)	6.15	0.230
Displacement	Δ (t)	8636.0	443.9
Displacement Volume	∇ (m^3)	8425.4	0.443
Wetted Surface	S (m^2)	2949.5	4.14

full-scale ship, but it is widely used in towing tanks as a benchmark model for CFD validation of ship hydrodynamics problems.

The computations were performed for the DTMB-5415 hull for a scale ratio of 26.69.

3.2. Calculation domain

Due to the symmetry of the ship hull, only half of the ship hull is modeled, which allows a smaller number of cells in the calculation domain, faster calculation, and easy convergence. The domain dimensions were selected to mimic the influence of possible reflected waves from side boundaries. Calculation domain dimensions were selected as follows: 2.2 ship length forward, 2.5 ship length aft, and one ship length side (Figure 4).

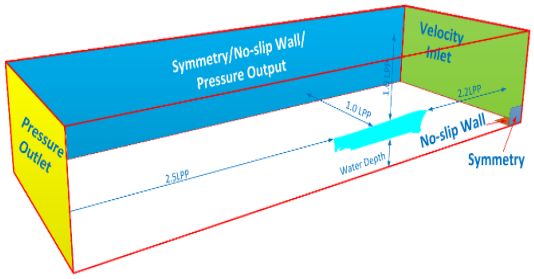

Figure 4. Calculation domain and boundary conditions

3.3. Numerical grids and time step

A numerical mesh was generated according to the considered water depth. A hexahedral mesh was used to achieve accurate predictions. To capture the exact flow at the hull surface, prism layer mesh was used. Besides, the refinements of the computational mesh were adopted, using volumetric controls with specific shapes for the considered regions in the flows near the hull surface. The accuracy of the CFD solution depends on the number of cells in the mesh. The optimal mesh is usually non-uniform: finer areas where the deviations from point to point are larger, and coarser areas where the variations are relatively small. For this purpose, finer meshes were created in the stern and bow areas where water disturbances occur, especially the free surface. In the recent research, 2.59 million cells mesh were used with water depth being 2 times the ship draft.

In addition, the movement of the vessel in shallow water often entails large changes in the floating position, requiring the use of suitable mesh techniques. One of the suitable mesh techniques is "morphing mesh", which allows the mesh to be deformed at a level relative to the original while preserving the connectivity of the elements.

The time step can be selected following ITTC recommendation: Δt=0.005 - 0.01L/V, where L is the ship length, V is the model speed. In this research, the time step Δt=0.035L/V was selected as the result of a convergence study carried out by Tezdogan [7].

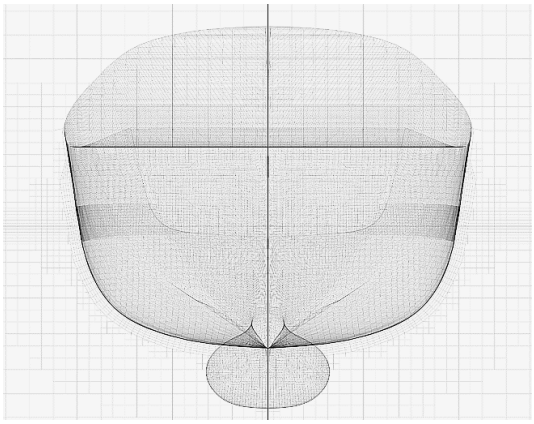

Figure 5. Calculation mesh

3.4. Boundary conditions

The boundary conditions for the simulation were set following widely used recommendations and research, as shown in Figure 4. The effect of the seabed on the hydrodynamics of the ship was taken

into account by setting the boundary condition as "moving no-slip wall" for the bottom of the calculation domain.

3.5. Physical models

For the simulation, the following physical models were selected: Implicit unsteady, Eulerian Multiphase, Volume of Fluid, Turbulent, K-Omega Turbulence, VOF Waves, Volume of Fluid.

The VOF wave damping was used as a remedy for wave reflections, which may occur and must be avoided as they may interact with the actual wave field and lead to invalid results. There are two causes of wave reflections: Wave reflections at edges and wave reflections due to abrupt mesh transitions.

For the simulation, a two-degree-of-freedom equilibrium motion was selected, including pitch and roll motion. For faster convergence and higher accuracy, according to the ship speed, the initial ship model will be moved and rotated to achieve a similar floating position to the model test results.

4. Result & convergence

The simulation was performed at various speeds as shown in Table 2.

Table 2. Calculation speeds

Speed (m/s)	F_h	Fr
0.597	0.281	0.083
0.799	0.376	0.111
0.995	0.468	0.138
1.199	0.564	0.166
1.291	0.608	0.179

The wave pattern at 0.799 m/s is shown in Figure 6.

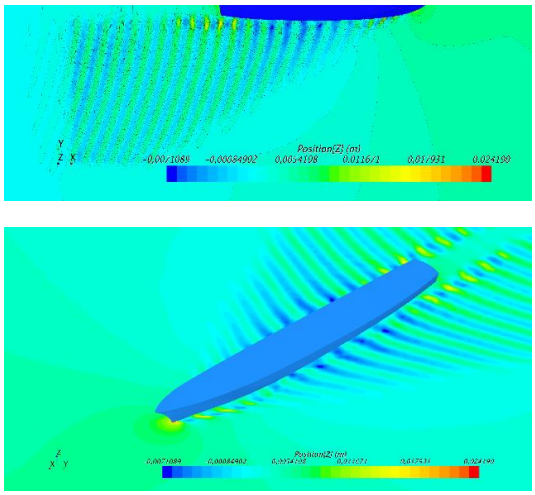

Figure 6. Wave pattern at 0.799 m/s (h/T = 2.0)

For comparison with shallow water experimental resistance values, which were obtained from the resistance test of the model DTMB M992 in the CTO towing tank, were taken. Resistance comparison with experiments is shown in Table 3.

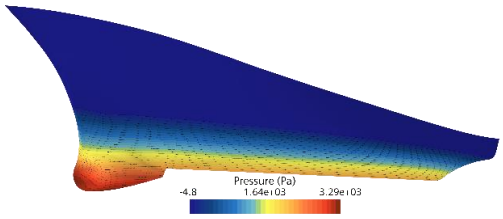

Figure 7. Pressure on ship hull at 0.799 m/s (h/T = 2.0)

Table 3. Resistance comparision with experiments

Speed (m/s)	EFD (N)	CFD (N)	Error, %
0.597	4.67	4.81	3.0%
0.799	7.28	7.55	3.7%
0.995	10.67	11.10	4.1%
1.199	15.29	15.78	3.2%
1.291	16.70	17.48	4.7%

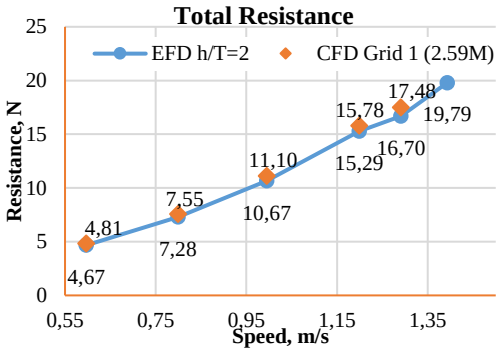

Figure 8. Resistance comparison with experiments

The shallow water resistance taken by the model test compared with the simulation result shows a good agreement.

The mesh quality is crucial factor that affects the convergence and accuracy of the simulation. A number of runs of a model with increasing levels of mesh refinement in the areas of interest can be used to demonstrate mesh convergence.

Theoretically, mesh convergence may be performed by an analysis of a critical parameter (resistance) in a specific location against mesh size. In the absence of experimental data, the ITTC guidance recommends the analysis of three mesh sizes [8]. In case of simulation results from two different mesh

TẠP CHÍ ISSN: 1859-316X, e-ISSN: 3093-3161
KHOA HỌC CÔNG NGHỆ HÀNG HẢI
JOURNAL OF MARINE SCIENCE AND TECHNOLOGY

sizes match each other, convergence can be considered to be achieved, and there is no need to generate a convergence analysis.

5. Conclusion

The result of ship resistance at shallow water (h/T = 2.0) by using CFD and experiments shows a good agreement with the experimental data. The error varies from 3.0% to 4.7% over sub-critical and near-critical speed ranges.

The present study shows the applicability of CFD method to numerically simulate the resistance of ship in shallow water with the implementation of the "morphing mesh" technique.

Further application of the "overset mesh" technique will be investigated for comparison of accuracy level with the above applied mesh technique.

Acknowledgements

This research is funded by Vietnam Maritime University under grant number: **DT24-25.30**.

REFERENCES

[1] Petros Voxakis (2012), *Ship Hull Resistance Calculation Using CFD Methods*, MIT.

[2] Pritam Kumar Patel, M. Prechand (2015), *Numerical Investigation of the Influence of Water Depth on Ship Resistance, Naval Architecture & Ocean Engineering Idian Maritime University*, National Ship Design & Research Centre Visakhapatnam.

[3] Senthil Prakash M. N, Binod Chandra (2013). *Numerical Estimation of Shallow Water Resistance of a River-Sea Ship using CFD*. International Journal of Computer Applications.

[4] Anthony F. Molland, Stephen R. Turnock, Dominic A (2011). *Hudson, Ship Resistance and Propulsion*, University of Southampton.

[5] Zhirong Zhang, Chengsheng Wu, Shaofeng Huang, Feng Zhao, Zhenping Weng (2010), *Numerical Simulation of Free Surface Flow of KCS and the Interaction between Propeller and Hull*, Gothenburg.

[6] Chengsheng Wu, Lei Yang, Zhirong Zhang, Feng Zhao, Kai Yan (2010), *CFD Simulation of Ship Model Free Sinkage and Trim Advancing in Calm Water*, Gothenburg.

[7] Tezdogan, T., Incecik, A., Turan, O., (2016). *A numerical investigation of the squat and resistance of ships advancing through a canal using CFD*. J. Mar. Sci. Technol. Vol.21, pp.86-101.

[8] ITTC (2008)-Quality Manual 7.5-03-01-01.

Received:	10 April 2025
Revised:	22 April 2025
Accepted:	24 April 2025